Chapter 2
A numerical approach based on Vieta-Fibonacci polynomials to solve fractional order advection-reaction diffusion problem

2.1 Introduction

The advection reaction-diffusion equation is widely used in science and engineering as a mathematical model in different areas such as transportation in porous media, oil reservoir simulation, global weather prediction, transport of mass and energy, and chemical transformation. The solute spreads within the fluid by molecular diffusion. The random collision of the solute molecule with the fluid molecule causes diffusion and produces a flux from the higher concentrated areas to the lower concentrated areas. The advective term describes the bulk movement of solute particles in the direction of fluid flow at a rate equal to fluid velocity. In addition to advective transport, solute spreads within the fluid in the porous medium by molecular diffusion. The mathematical models related to the mixture of the advective and reactive processes can be seen in various directions in real life, for instance, dynamics of age-structured populations, in meteorological pollution control models, etc. Despite all these, we face great complications when the model of advection-reaction-diffusion is nonlinear. Physical phenomena like fast diffusion or slow diffusion are very much relevant for the porous media. In recent years, the theory of fractional calculus has

attracted by many researchers due to its numerous applications in various fields, like image processing [59] , mathematics and physics [60], economics [61]-[62], fluid dynamics [63], control theory [64], fracture mechanics [65], etc. In 2022, Baleanu et al. [66] used Caputo fractional derivative to present a general mathematical model for a real situation of the cholera outbreak. Defterli et al. [67] also discussed the application of fractional calculus in an accelerated mass-spring system, and presented the fractional Euler-Lagrange equations. Some definitions and properties of fractional calculus can be seen in the book of Abbas et al. [68]. Jajarmi et al. [69] recently presented a regularized $\Psi-$Hilfer fractional derivative and its properties. They presented the application of this generalized fractional derivative for an initial-value problem, and its solution is also analyzed.

The advection-reaction diffusion equations with fractional derivatives play an important role to describe the anomalous transport dynamics in a heterogeneous media, and is a useful tool for modelling many physical problems of surface water pollution, ground water pollution, and atmospheric pollution, which directly affects the health of the human being. Therefore, in the last few decades, fractional advection-reaction diffusion equations have drawn a great attraction to a lot of researchers. In the literature of advection-diffusion equations with fractional derivatives, several mathematical models have been presented by many authors, for example, Deng et al. [70] discussed one-dimensional (fractional advection-dispersion equation, and they developed stability criteria for the numerical schemes to solve fractional advection-dispersion equation. Jiang and Lin [71] discussed the fractional advection-dispersion equation with Caputo fractional time derivative and Riemann-Liouville (R-L) space fractional derivative, Lin et al. [72] presented a nonlinear diffusion equation with the Riesz fractional derivative, Pandey et al. [73] discussed a coupled advection reaction diffusion equations with time fractional derivative in Caputo sense for the

two interacting species in the domain of fluid flow through the porous medium, a mathematical model of advection reaction diffusion equations with time and space fractional in R-L sense is presented by Jannelli et al. [74], Ginting and Li [75] used the R-L derivatives in a mathematical model of one-dimensional double-sided diffusion-advection-reaction and established the existence, uniqueness, and regularity of the problem on the real line. Singh and Das [76] considered the Caputo fractional derivatives for both space and time in their study to present a model of fractional-order advection reaction diffusion equations, etc.

In general, the exact solutions of factional-order advection reaction diffusion equations are limited, therefore various numerical/approximate techniques have been used to solve these equations, like Adomian decomposition method [77], homotopy perturbation method [78], finite difference methods [79–82], homotopy perturbation transform method [83], [84], etc. Dwivedi and Das [85] presented a solution to a fractional-order Burger-Fisher-Fitzhugh-Nagumo equation by using the Fibonacci collocation and non-standard finite difference method. Heydari and Atangana [86] presented a numerical scheme based on Chebyshev cardinal functions and piecewise Chebyshev cardinal functions for solving a nonlinear advection reaction diffusion equations with the piecewise fractional derivatives. Sweilam et al. [87] presented a linear model of advection-dispersion problem with spatial fractional derivatives and discussed its solution with the help of spectral collocation method and non-standard finite difference scheme. In 2022, Abeye et al. [88] discussed the Laguerre spectral collocation and finite difference methods to solve the fractional advection dispersion equations. In 2023, Sharma and Rajeev [89], [90] solved advection reaction diffusion equations numerically and in the same year, Biswas et al. [91] discussed a shifted Legendre collocation method to solve a fractional-order nonlinear advection reaction diffusion equations.

In the study of nonlinear physical problems, fractional order reaction-advection-diffusion model plays a significant role, therefore the author is motivated to find the approximate numerical solution of space-time fractional order reaction-advection-diffusion equation and to analyses their physical behavior in porous media associated with Caputo fractional order derivatives. In the present scientific contribution, the author analyzed the mathematical form of a physical problem. Here author traces the behavior solute species under the influence of reaction, diffusion, and advection in porous media. Our main goal is to find the long-term behavior of the considered nonlinear system. Here we present a fractional nonlinear mathematical model of such a physical problem containing solute variables. In this chapter, author consider the fractional reaction advection diffusion equation [74], [87] in porous media as:

$$\frac{\partial^{\alpha} u}{\partial t^{\alpha}} = -a(x,t)\frac{\partial}{\partial x}\left(-\frac{\partial^{\gamma} u}{\partial x^{\gamma}}\right) - b(x,t)\frac{\partial^{\gamma} u}{\partial x^{\gamma}} + f(u,x,t), \quad x \in (0,1), \quad t \in (0,T), \tag{2.1}$$

with intial and boundary conditions

$$\begin{aligned} &u(x,0) = \xi_0(x), \quad x \in (0,1), \\ &u(0,t) = g_1(t), \quad u(1,t) = g_2(t), \quad t \in (0,T), \end{aligned} \tag{2.2}$$

where

$$0 < \alpha \leq 1, \qquad 1 < 1 + \gamma = \beta \leq 2, \qquad 0 < \gamma \leq 1,$$

and $a(x,t)$ is the dispersion coefficient, $b(x,t)$ is the average fluid velocity, u is the solute concentration, α is the order of the time-fractional derivative, γ is the space derivative of fractional-order. All the fractional derivatives are considered in Caputo sense. In the case α=γ=1, the above equation reduces to the classical

reaction-advection diffusion equation.

In this article, our main aim is to discuss a new approach that is the combination of non-standard finite difference method and spectral collocation scheme to solve a space-time fractional model of advection reaction diffusion equations with nonlinear terms as given in (2.1)-(2.2). The accuracy of the scheme is numerically verified for the two different examples, and it is shown that the proposed solution is sufficiently accurate. The stability and error estimates for the non-standard finite difference scheme are also analyzed. The presence of nonlinear coefficients and nonlinear source terms play an important role from the physical point of view as compared to a linear model. This motivates the authors to solve the considered nonlinear porous media problem.

This chapter is organised as follows: In section 2.2, the preliminaries are presented that consist of the basic of Caputo derivative of fractional-order and some properties of shifted Vieta-Fibonacci polynomials and shifted Chebyshev polynomial of the second kind. Section 2.3 includes the details of non-standard finite difference scheme. In section 2.4, we develop an approximate formula dimensions Caputo derivative of fractional-order for a function. Section 2.5 gives the numerical solution of the fractional reaction advection diffusion equations with the help of non-standard finite difference scheme and spectral collocation method. Section 2.6 describes the stability of the presented scheme. In section 2.7, some numerical examples and results are presented. The last section 2.8 presents the conclusion of the study.

2.2 Preliminaries and Definitions

Some definitions and characteristics of fractional calculus that are relevant to this chapter are explained in this section.

2.2.1 Shifted Vieta-Fibonacci Polynomials

The Vieta-Fibonacci polynomials ($\mathcal{VF}_n(x)$) is defined as

$$\mathcal{VF}_n(x) = \frac{(\sin(n)\varphi)}{\sin(\varphi)}, \qquad n \in \mathbb{N},$$

where $x = 2\cos\varphi$, $\varphi \in [0, \pi]$. The Vieta-Fibonacci polynomials can be generated by using the recurrence relation shown below.

$$\mathcal{VF}_n(x) = x\mathcal{VF}_{n-1}(x) - \mathcal{VF}_{n-2}(x), \quad n = 2, 3, ...,$$

with the conditions

$$\mathcal{VF}_0(x) = 0, \quad \mathcal{VF}_1(x) = 1.$$

As given in [87], the shifted Vieta-Fibonacci polynomial of degree n ($\mathcal{VF}^*_n(x)$) is defined in finite range [0,1] as follow

$$\mathcal{VF}^*_n(x) = \mathcal{VF}_n(4x - 2), \tag{2.3}$$

with the values

$$\mathcal{VF}^*_0(x) = 0, \quad \mathcal{VF}^*_1(x) = 1. \tag{2.4}$$

Additionally, using any one of the two following formulas, $\mathcal{VF}^*_n(x)$ can be produced in the power series formula:

$$\mathcal{VF}^*_n(x) = \sum_{i=0}^{n} (-1)^i \frac{2^{2n-2i-2}\Gamma(2n-i)}{\Gamma(i+1)\Gamma(2n-2i)} x^{n-i-1}, \quad n \in \mathbb{Z}^+, \tag{2.5}$$

or

$$\mathcal{VF}_n^*(x) = \sum_{i=0}^{n}(-1)^{n-i-1}\frac{2^{2i}\Gamma(n+i+1)}{\Gamma(n-i)\Gamma(2i+2)}x^i, \quad n \in \mathbb{Z}^+. \tag{2.6}$$

The polynomials $\mathcal{VF}_n^*(x)$ are orthogonal with respect to weight function $\omega(x) = \sqrt{x-x^2}$ as

$$\langle \mathcal{VF}_{n_1}^*(x), \mathcal{VF}^* n_2(x)\rangle = \int_0^1 \omega(x)\mathcal{VF}_{n_1}^*(x)\mathcal{VF}_{n_2}^*(x)dx, \begin{cases} 0, & n_1 \neq n_2, \\ \frac{\pi}{8}, & n_1 = n_2 \neq 0. \end{cases} \tag{2.7}$$

Now, suppose the approximate solution $\chi(x) \in L^2[0,1]$, then it can be expressed in terms of the shifted Vieta-Fibonacci polynomials as

$$\chi(x) = \sum_{i=1}^{\infty} U_i \mathcal{VF}_i^*(x), \tag{2.8}$$

where U_i are the unknown coefficients. For the practical applications, we take finite terms ($(m+1)$ terms) of shifted Vieta-Fibonacci polynomials in the (2.8) as given below

$$\chi_m(x) = \sum_{i=1}^{m+1} U_i \mathcal{VF}_i^*(x), \tag{2.9}$$

where the unknown coefficients vector $U_i(i = 1, 2, 3, ..., m+1)$ can be obtained through any of the following relation:

$$U_i = \frac{1}{2\pi}\int_{-2}^{2} \chi(\frac{x+2}{4})\sqrt{4-x^2}\mathcal{VF}_i(x)dx, \tag{2.10}$$

or

$$U_i = \frac{8}{\pi}\int_0^1 \chi(x)\sqrt{x-x^2}\mathcal{VF}_i^*(x)dx. \tag{2.11}$$

2.2.2 Shifted Chebyshev Polynomials of the Second Kind

The chebyshev polynomials of the second kind $\mathcal{U}_n(x)$ are orthogonal polynomials of degree n in x defined on [-1,1] and these polynomials is given by

$$\mathcal{U}_n(x) = \frac{\sin(x+1)\varphi}{\sin\varphi}, \tag{2.12}$$

where $x = \cos\varphi$ and $\varphi \in [0, \pi]$.

Also $\mathcal{U}_n(x)$ satisfy the following recurrence formula

$$\mathcal{U}_n^*(x) = (4x-2)\mathcal{U}_{n-1}^*(x) - \mathcal{U}_{n-2}^*(x), \quad n = 2, 3, ..., \tag{2.13}$$

with the starting values

$$\mathcal{U}_0^*(x) = 1, \;\; \mathcal{U}_0^*(x) = 4x - 2. \tag{2.14}$$

Moreover, $\mathcal{U}_n^*(x)$ have analytical form given as follows:

$$\mathcal{U}_n^*(x) = \sum_{i=0}^{n} (-1)^i \frac{2^{2n-2i}\Gamma(2n-i+2)}{\Gamma(i+1)\Gamma(2n-2i+2)} x^{n-i}, \quad n \in \mathbb{Z}^+. \tag{2.15}$$

$\mathcal{U}_n^*(x)$ are orthogonal on the interval [0,1] as given below

$$\langle \mathcal{U}_{n_1}^*(x), \mathcal{U}^* n_2(x) \rangle = \int_0^1 \sqrt{x - x^2}\, \mathcal{U}_{n_1}^*(x) \mathcal{U}_{n_2}^*(x) dx, \begin{cases} 0, & n_1 \neq n_2, \\ \frac{\pi}{8}, & n_1 = n_2 \neq 0. \end{cases} \tag{2.16}$$

2.3 Non-Standard Finite Difference Scheme

In this section, we would like to introduce non-standard finite difference schemes, which was firstly introduced by Mickens [57]. In this method, the first derivative is approximated as

$$\frac{du}{dt} \to \frac{u_{h+1} - \varpi(k)u_h}{x(k)},$$

where $\varpi(k)$ and $x(k)$ are two continuous functions of step-size k, that satisfies both conditions listed below:

$$\varpi(k) = 1 + O(k^2) \; and \; x(k) = h + O(k^2).$$

Moreover, the continuous function $x(k)$ satisfies the condition $0 < x(k) < 1$, $k \to 0$. Examples of such functions are

$$\varpi(k) = e^k - 1, \quad \varpi(k) = k,$$

$$x(k) = sinh(k), \quad x(k) = \frac{1 - e^{-\lambda k}}{\lambda}, etc.$$

.

There is no specific principle to choose the best function $x(k)$.

2.4 Appoximation of Caputo Derivative for Fractional-Order

Theorem 2.1. *If the appoximate solution $\chi_m(x)$ of the problem (2.1)-(2.2) is expreesed as given in Equation (2.9), then the space fractional derivative for $\chi_m(x)$ is*

given by

$$D_x^{\mu}(\chi_m(x)) = \sum_{i=\lceil \mu \rceil}^{m+1} \sum_{k=\lceil \mu \rceil}^{i} U_i \ \eta_{i,k}^{\mu} \ x^{k-\mu}, \tag{2.17}$$

where

$$\eta_{i,k}^{\mu} = \frac{(-1)^{i-k-1}(2)^{2k}\Gamma(i+k+1)\Gamma(k+1)}{\Gamma(i-k)\Gamma(2k+2)\Gamma(k+1-\mu)}. \tag{2.18}$$

Proof Let us apply the Caputo fractional differential operator (D^{μ}) to the approximate solution of the problem (2.1)-(2.2), we get

$$D_x^{\mu}(\chi_m(x)) = \sum_{i=1}^{m+1} U_i D^{\mu}(\mathcal{VF}_i^*(x)). \tag{2.19}$$

According to the properties of Caputo fractional derivatives as given in chapter 1, we have

$$D_x^{\mu}(\mathcal{VF}_i^*(x)) = 0, \quad i = 1, 2, ...\lceil \mu \rceil - 1, \tag{2.20}$$

and

$$D_x^{\mu}(\mathcal{VF}_i^*(x)) = \sum_{k=0}^{i} \frac{(-1)^{i-k-1}(2)^{2k}\Gamma(i+k+1)}{\Gamma(i-k)\Gamma(2k+2)} D^{\mu}(x^k). \tag{2.21}$$

From the definition of Caputo derivatives given in chapter 1 and equations (2.20)-(2.21), we get

$$D_x^{\mu}(\mathcal{VF}_i^*(x)) = \sum_{k=\lceil \mu \rceil}^{i} \frac{(-1)^{i-k-1}(2)^{2k}\Gamma(i+k+1)\Gamma(k+1)}{\Gamma(i-k)\Gamma(2k+2)\Gamma(k+1-\mu)} x^{k-\mu}. \tag{2.22}$$

Substituting equation (2.22) into equation (2.19) and using equation (2.21), we obtain

$$D_x^{\mu}(\chi_m(x)) = \sum_{i=\lceil \mu \rceil}^{m+1} \sum_{k=\lceil \mu \rceil}^{i} U_i \frac{(-1)^{i-k-1}(2)^{2k}\Gamma(i+k+1)\Gamma(k+1)}{\Gamma(i-k)\Gamma(2k+2)\Gamma(k+1-\mu)} x^{k-\mu}, \tag{2.23}$$

Here, equation (2.23) can be restated as

$$D_x^{\mu}(\chi_m(x)) = \sum_{i=\lceil\mu\rceil}^{m+1} \sum_{k=\lceil\mu\rceil}^{i} U_i \ \eta_{i,k}^{\mu} \ x^{k-\mu}, \tag{2.24}$$

where,

$$\eta_{i,k}^{\mu} = \frac{(-1)^{i-k-1}(2)^{2k}\Gamma(i+k+1)\Gamma(k+1)}{\Gamma(i-k)\Gamma(2k+2)\Gamma(k+1-\mu)}. \tag{2.25}$$

This proof is based on [87].

Moreover, the fractional derivative of an approximated function $\chi_m(x)$ in terms of the shifted chebyshev polynomials of second kind is derived in [92].

2.5 Solution of the Problem

To solve the FRADE given in (2.1)-(2.2) with the help of shifted Vieta-Fibonacci collocation method (SVFCM), let us take the following approximation for $u_m(x,t)$ in terms of $\mathcal{VF}^*(x)$ as given in [87]

$$u_m(x,t) = \sum_{i=1}^{m+1} U_i(t)\mathcal{VF}_i^*(x). \tag{2.26}$$

Substituting the approximation of $u_m(x,t)$ in equation (2.1), we get

$$\begin{aligned} \sum_{i=1}^{m+1} \frac{d^{\alpha}U_i(t)}{dt^{\alpha}} V F_i^*(x) &= a\,(x,t) \left(\sum_{i=1}^{m+1} D^{\beta}\mathcal{VF}_i^*(x)U_i(t) \right) \\ - b\,(x,t) \sum_{i=1}^{m+1} D^{\gamma}\mathcal{VF}_i^*(x)U_i(t) &+ f\left(\sum_{i=1}^{m+1} U_i(t)\mathcal{VF}_i^*(x), x, t \right). \end{aligned} \tag{2.27}$$

Using theorem (2.1), we can rewrite the preceding equation as

$$\sum_{i=1}^{m+1} \frac{d^{\alpha} U_i(t)}{dt^{\alpha}} \mathcal{VF}_i^*(x) = a\,(x,t) \left(\sum_{i=\lceil \beta \rceil}^{m+1} \sum_{k=\lceil \beta \rceil}^{i} U_i(t)\ \eta_{i,k}^{\beta}\ x^{k-\beta} \right)$$
$$- b\,(x,t) \left(\sum_{i=\lceil \gamma \rceil}^{m+1} \sum_{k=\lceil \gamma \rceil}^{i} U_i(t)\ \eta_{i,k}^{\gamma}\ x^{k-\gamma} \right) + f\left(\sum_{i=1}^{m+1} U_i(t) \mathcal{VF}_i^*(x), x, t \right), \qquad (2.28)$$

where $\quad 0 < x < 1, \quad 0 < t \leq T, \quad 0 < \alpha \leq 1.$

The boundary conditions can be written as

$$\sum_{i=1}^{m+1} U_i(t) \mathcal{VF}_i^*(0) = g_1(t),$$
$$\sum_{i=1}^{m+1} U_i(t) \mathcal{VF}_i^*(1) = g_2(t). \qquad (2.29)$$

To solve the partial differential equation (2.28), the non-standard finite difference scheme is used. For this purpose, first, we discretize the time fractional derivative by dividing the time interval into M parts and we take $t_n = n\Delta t,\ \Delta t = t_{j+1} - t_j,\ j = 0, 1, ..., n-1,\ n = 0, 1, ..., M$. Here, the value of $U_i(t)$ at point $t = t_n$ is denoted by U_i^n.

Now, by using the Caputo's definition for time derivative, we have

$$\begin{aligned} \frac{d^{\alpha} U_i(t_n)}{dt^{\alpha}} &= \frac{1}{\Gamma(1-\alpha)} \int_0^{t_n} (t_n - s)^{-\alpha} \frac{dU_i}{ds} ds, \\ &= \frac{1}{\Gamma(1-\alpha)} \sum_{j=0}^{n-1} \frac{U_i^{j+1} - U_i^j}{\phi(\Delta t)} \int_{t_j}^{t_j+1} (t_n - s)^{-\alpha} ds, \\ &= \frac{1}{\Gamma(2-\alpha)} \sum_{j=0}^{n-1} \frac{U_i^{j+1} - U_i^j}{\phi(\Delta t)} [(t_n - t_j)^{1-\alpha} - (t_n - t_{j+1})^{1-\alpha}]. \end{aligned} \qquad (2.30)$$

Considering the fractional partial differential equation (2.28) at the point $t = t_n$ and using equation (2.30), we get the following set of non-linear algebraic equations:

$$\begin{aligned}\frac{1}{\Gamma(2-\alpha)}\sum_{i=1}^{m+1}\sum_{j=0}^{n-1}\frac{U_i^{j+1}-U_i^j}{\phi(\Delta t)}[(t_n-t_j)^{1-\alpha}-(t_n-t_{j+1})^{1-\alpha}]\mathcal{VF}_i^*(x)\\ = a\,(x,t_n)\left(\sum_{i=\lceil\beta\rceil}^{m+1}\sum_{k=\lceil\beta\rceil}^{i}U_i^n\;\eta_{i,k}^{\beta}\;x^{k-\beta}\right)\\ - b\,(x,t_n)\left(\sum_{i=\lceil\gamma\rceil}^{m+1}\sum_{k=\lceil\gamma\rceil}^{i}U_i^n\;\eta_{i,k}^{\gamma}\;x^{k-\gamma}\right)\\ + f\left(\sum_{i=1}^{m+1}U_i^n\mathcal{VF}_i^*(x),x,t_n\right).\end{aligned}\tag{2.31}$$

Also, the boundary conditions at the points $t = t_n$ becomes

$$\sum_{i=1}^{m+1}U_i^n\mathcal{VF}_i^*(0)=g_1(t_n),\tag{2.32}$$

$$\sum_{i=1}^{m+1}U_i^n\mathcal{VF}_i^*(1)=g_2(t_n).\tag{2.33}$$

Now, we collocate equations (2.31), (2.32) and (2.33) at the root of $\mathcal{VF}^*_{m+2-\lceil\beta\rceil}(x_p)$ which, respectively give

$$\begin{aligned}\frac{1}{\Gamma(2-\alpha)}\sum_{i=1}^{m+1}\sum_{j=0}^{n-1}\frac{U_i^{j+1}-U_i^j}{\phi(\Delta t)}[(t_n-t_j)^{1-\alpha}-(t_n-t_{j+1})^{1-\alpha}]\mathcal{VF}_i^*(x_p)\\ = a\,(x_p,t_n)\left(\sum_{i=\lceil\beta\rceil}^{m+1}\sum_{k=\lceil\beta\rceil}^{i}U_i^n\;\eta_{i,k}^{\beta}\;x_p^{k-\beta}\right)\\ - b\,(x_p,t_n)\sum_{i=\lceil\gamma\rceil}^{m+1}\sum_{k=\lceil\gamma\rceil}^{i}U_i^n\;\eta_{i,k}^{\gamma}\;x_p^{k-\gamma}\\ + f\left(\sum_{i=1}^{m+1}U_i^n\mathcal{VF}_i^*(x_p),x_p,t_n\right),\end{aligned}\tag{2.34}$$

where $p = 1, 2, ..., (m + 1 - \lceil\beta\rceil)$,

$$\sum_{i=1}^{m+1} U_i^n \mathcal{VF}_i^*(0) = g_1(t_n), \tag{2.35}$$

and

$$\sum_{i=1}^{m+1} U_i^n \mathcal{VF}_i^*(1) = g_2(t_n). \tag{2.36}$$

To find the initial approximation, the following initial condition is considered

$$\sum_{i=1}^{m+1} U_i^0 \mathcal{VF}_i^*(x_p) = \xi_0(x_p). \tag{2.37}$$

The equation (2.34) generates a system of $(m + 1 - \lceil\beta\rceil)$ algebraic equations. In views of equations (2.35)-(2.36), this system of algebraic equations reduces to a new system of $(m+1)$ algebraic equations with $(m+1)$ unknowns. By solving this new system, we get the value of unknowns.

In order to find the solution of (2.1)-(2.2) with the help of Chebyshev collocation method (CCM), first we express $u_m(x,t)$ in terms of $\mathcal{U}^*(x)$. After that by using [92], the Eqs. (2.1)-(2.2) can be written in the following form

$$\begin{aligned}
\frac{1}{\Gamma(2-\alpha)} \sum_{i=0}^{m} \sum_{j=0}^{n-1} \frac{U_i^{j+1} - U_i^j}{\phi(\Delta t)} [(t_n - t_j)^{1-\alpha} - (t_n - t_{j+1})^{1-\alpha}] \mathcal{U}_i^*(x) \\
= a\,(x, t_n) \left(\sum_{i=\lceil\beta\rceil}^{m} \sum_{k=\lceil\beta\rceil}^{i} U_i^n \ \eta_{i,k}^{\beta} \ x^{k-\beta} \right) \\
- b\,(x, t_n) \left(\sum_{i=\lceil\gamma\rceil}^{m} \sum_{k=\lceil\gamma\rceil}^{i} U_i^n \ \eta_{i,k}^{\gamma} \ x^{k-\gamma} \right) \\
+ f \left(\sum_{i=0}^{m} U_i^n \mathcal{U}_i^*(x), x, t_n \right),
\end{aligned} \tag{2.38}$$

$$\sum_{i=0}^{m} U_i^n \mathcal{U}_i^*(0) = g_1(t_n), \tag{2.39}$$

$$\sum_{i=0}^{m} U_i^n \mathcal{U}_i^*(1) = g_2(t_n), \tag{2.40}$$

$$\sum_{i=0}^{m} U_i^0 \mathcal{U}_i^*(x) = \xi_0(x). \tag{2.41}$$

Now, collocating equation (2.38)-(2.41) at the root of $\mathcal{U}^*_{m+1-\lceil\beta\rceil}(x_p)$ generates a system of algebraic equations. By solving this generated system, we can find the value of unknowns.

2.6 Stability and Convergence Analysis

Let us consider the following problem [85] with fractional time derivative to discuss the stability and error estimate of our proposed scheme

$$\frac{\partial^\alpha u}{\partial t^\alpha} = a(x,t)\frac{\partial^2 u}{\partial x^2} - b(x,t)\frac{\partial u}{\partial x} + u(x,t) + f(x,t) \tag{2.42}$$

with the conditions

$$u(0,t) = 0, \quad u(1,t) = 0,$$

where $a(x,t)$ and $b(x,t)$ are the positive functions. Clearly Eq. (2.42) is a particular of (2.1)-(2.2).

From the Eq. (2.34), we take the following approximation for the time fractional derivative by assuming $\phi(\Delta t) = \Delta t$

$${}_0^c D_t^\alpha u(x,t_{n+1}) = \frac{(\Delta t)^{-\alpha}}{\Gamma(2-\alpha)} \sum_{j=0}^{n} \vartheta_j [u(x,t_{n-j+1}) - u(x,t_{n-j})] + R_{n+1}^\alpha, \tag{2.43}$$

where $\vartheta_j = (j+1)^{1-\alpha} - j^{1-\alpha}$ and R^{α}_{n+1} is the truncation error which satisfies the following relation [82]

$$|R^{\alpha}_{n+1}| \leq C(\Delta t)^{2-\alpha}, \tag{2.44}$$

where C is a positive constant.

Substituting Equation (2.43) into Equation (2.44), we obtain

$$\begin{aligned} &u(x,t_{n+1}) - \rho\left[a(x,t_{n+1})\frac{\partial^2 u(x,t_{n+1})}{\partial x^2} - b(x,t_{n+1})\frac{\partial u(x,t_{n+1})}{\partial x}\right] \\ &= u(x,t_n) - \sum_{j=1}^{n}\vartheta_j[u(x,t_{n-j+1}) - u(x,t_{n-j})] + \rho u(x,t_{n+1}) + \rho f(x,t_{n+1}) + R_{n+1}, \end{aligned} \tag{2.45}$$

where

$$\rho = (\Delta t)^{\alpha}\Gamma(2-\alpha), \qquad |R_{n+1}| \leq C'(\Delta t)^2,$$

and the C' is a positive constant.

For the simplicity, let us consider the following notations

$$\begin{aligned} &u(x,t_{n+1}) \simeq u^{n+1}, \quad a(x,t_{n+1}) \simeq a^{n+1}, \quad b(x,t_{n+1}) \simeq b^{n+1}, \quad f(x,t_{n+1}) \simeq f^{n+1}, \\ &\frac{\partial^2 u(x,t_{n+1})}{\partial x^2} \simeq u^{n+1}_{xx}, \quad \frac{\partial u(x,t_{n+1})}{\partial x} \simeq u^{n+1}_{x}. \end{aligned}$$

Now, the Eq.(2.45) can be written in the following manner:

$$u^{n+1} - \rho\left[a^{n+1}u^{n+1}_{xx} - b^{n+1}u^{n+1}_{x}\right] = u^n - \sum_{j=1}^{n}\vartheta_j[u^{n-j+1} - u^{n-j}] + \rho u^{n+1} + \rho f^{n+1}, \tag{2.46}$$

where the coefficients of ϑ_j satisfies the following relation as reported in [82]

$$\begin{aligned}
&\vartheta_j > 0, \quad j = 0, 1, ..., n, \\
&\vartheta_0 > \vartheta_1 > ... > \vartheta_n, \quad \vartheta_n \to 0 \ \ as \ \ n \to \infty, \\
&\sum_{j=0}^{n} [\vartheta_j - \vartheta_{j+1}] + \vartheta_{n+1} = \vartheta_0 = 1.
\end{aligned}$$

Let us write the Eq. (2.46) as

$$\begin{aligned}
&(1-\rho)u^{n+1} - \rho\left[a^{n+1}u_{xx}^{n+1} - b^{n+1}u_x^{n+1}\right] \\
&\qquad = (1-\vartheta_1)u^n - \sum_{j=1}^{n-1}(\vartheta_{j+1} - \vartheta_j)u^{n-j} + \vartheta_n u^0 + \rho f^{n+1}. \qquad (2.47)
\end{aligned}$$

For this scheme, we have the following results.

Theorem 2.2. *Suppose* $u^n(x)$, $n = 0, 1, ..., N$, *is the solution of Eq.* (2.47) *and* $u^n(0)$=$u^n(1)$=*0, then*

$$\|u^n\|_2 \leq \|u^0\|_2 + \rho\vartheta_{n-1}^{-1} \max_{\{0<\iota<N\}} \|f^\iota\|_2.$$

Proof To prove this, we use the principal of mathematical induction as given in [81]-[80]. For $n = 0$, Eq. (2.47) gives

$$u^1 - \rho\left[a^1 u_{xx}^1 - b^1 u_x^1\right] = u^0 + \rho f^1.$$

Now, multiplying the above Equation by u^1 and integrating it over the interval $[0, 1]$ and utilizing the definition of the inner product, we get

$$(1-\rho)\langle u^1, u^1\rangle - \rho[a^1\langle u_{xx}^1, u^1\rangle - b^1\langle u_x^1, u^1\rangle] = \langle u^0, u^1\rangle + \rho\langle f^1, u^1\rangle. \qquad (2.48)$$

Now, using the following relations

$$\langle u_{xx}^1, u^1\rangle = -\|\frac{\partial u^1}{\partial x}\|_2^2, \quad \langle u_x^1, u^1\rangle = 0,$$

in the Eq. (2.48), we get

$$(1-\rho)\|u^1\|_2^2 + \rho a^1 \|\frac{\partial u^1}{\partial x}\|_2^2 = \langle u^0, u^1\rangle + \rho\langle f^1, u^1\rangle.$$

Using the Schwarz ineqality and ϑ_0^{-1}=1 in the above equation, we get

$$(1-\rho)\|u^1\|_2 \leq \|u^0\|_2 + \rho\vartheta_0^{-1} \max_{\{0<\iota<N\}} \|f^\iota\|_2.$$

If Δt is a small quantity, then we get

$$\|u^1\|_2 \leq \|u^0\|_2 + \rho\vartheta_0^{-1} \max_{\{0<\iota<N\}} \|f^\iota\|_2. \tag{2.49}$$

Now, we assume that

$$\|u^j\|_2 \leq \|u^0\|_2 + \rho\vartheta_{j-1}^{-1} \max_{\{0<\iota<N\}} \|f^\iota\|_2, \quad j = 1, 2, ..., n. \tag{2.50}$$

Multiplying both sides of eq. (2.47) by u^{n+1} and integrating over the interval $[0, 1]$, we obtain

$$\begin{aligned}(1-\rho)\langle u^{n+1}, u^{n+1}\rangle - \rho[a^{n+1}\langle u_{xx}^{n+1}, u^{n+1}\rangle - b^{n+1}\langle u_x^{n+1}, u^{n+1}\rangle] \\ = (1-\vartheta_1)\langle u^n, u^{n+1}\rangle - \sum_{j=1}^{n-1}[\vartheta_{j+1} - \vartheta_j]\langle u^{n-j}, u^{n+1}\rangle + \vartheta_n\langle u^0, u^{n+1}\rangle + \rho\langle f^{n+1}, u^{n+1}\rangle,\end{aligned}$$

and by using Schwartz's inequality, we get

$$(1-\rho)\|u^{n+1}\|_2 \leq (1-\vartheta_1)\|u^n\|_2 - \sum_{j=1}^{n-1}[\vartheta_{j+1}-\vartheta_j]\|u^{n-j}\|_2 + \vartheta_n\|u^0\|_2 + \rho\|f^{n+1}\|_2.$$

From Eq. (2.50) and $\vartheta_{j+1}^{-1} \geq \vartheta_j^{-1}$ for $j = 0, ..., n$ as given in [80], we have

$$\begin{aligned}(1-\rho)\|u^{n+1}\|_2 \leq (1-\vartheta_1)&\left[\|u^0\|_2 + \rho\vartheta_{n-1}^{-1}\max_{\{0<\iota<N\}}\|f^\iota\|_2\right] \\ &- \sum_{j=1}^{n-1}[\vartheta_{j+1}-\vartheta_j]\left[\|u^0\|_2 + \rho\vartheta_{n-j-1}^{-1}\max_{\{0<\iota<N\}}\|f^\iota\|_2\right] \\ &+ \vartheta_n\|u^0\|_2 + \rho\|f^{n+1}\|_2.\end{aligned}$$

As $\Delta t \to 0$, $(1-\rho) \to 1$ so, we get

$$\|u^{n+1}\|_2 \leq \left[\|u^0\|_2 + \rho\vartheta_n^{-1}\max_{\{0<\iota<N\}}\|f^\iota\|_2\right]. \tag{2.51}$$

Theorem 2.3. *The semi discretized problem (2.47) is unconditionally stable.*

Proof Suppose $\widetilde{u}^n(x)$ is the approximate solution of (2.47).

Let us take $\varepsilon^n = u^n(x) - \widetilde{u}^n(x)$. Therefore, from eq. (2.47), we have

$$(1-\rho)\varepsilon^{n+1} - \rho[a^{n+1}\varepsilon_{xx}^{n+1} - b^{n+1}\varepsilon_x^{n+1}] = (1-\vartheta_1)\varepsilon^n - \sum_{j=1}^{n-1}(\vartheta_{j+1}-\vartheta_j)\varepsilon^{n-j} + \vartheta_n\varepsilon^0. \tag{2.52}$$

Since $\varepsilon^{n+1}|_0^1 = 0$, so from the Theorem 2.2, we get

$$\|\varepsilon^n\|_2 \leq \|\varepsilon^0\|_2, \qquad n = 1, 2, ..., N. \tag{2.53}$$

Theorem 2.4. *Suppose* $u(x,t_n)$ *and* $\{u^n(x)\}_{n=0}^N$ *are the exact and time-discrete solutions of the Eq.* (2.1)*, respectively. Let us assume that* $u(x,0)=u^0(x)$*, then*

$$\|u(x,t_n)-u^n\|_2 \leq \widetilde{C}(\Delta t)^{2-\alpha}, \qquad 0<\alpha<1,$$

where $\widetilde{C}$ *is a positive constant.*

Proof Let $\epsilon^n = u(x,t_n)-u^n(x)$.

From eq. (2.45) and (2.47), we have

$$(1-\rho)\epsilon^{n+1}-\rho\left[a^{n+1}\epsilon_{xx}^{n+1}-b^{n+1}\epsilon_x^{n+1}\right]=(1-\vartheta_1)\epsilon^n-\sum_{j=1}^{n-1}(\vartheta_{j+1}-\vartheta_j)\epsilon^{n-j}+\vartheta_n\epsilon^0+R_{n+1},$$

with $\epsilon^0(x)=0$.

Using Theorem 2.3 and [81] in the above equation, we get

$$\|\epsilon^n\|_2 \leq \widetilde{C}(\Delta t)^{2-\alpha}.$$

2.7 Numerical Results

In this section, we present the numerical results associated with the equations (2.1)-(2.2) with the aid of technique which is discussed in the section 2.5. We consider the following two examples to compare our results with the exact solutions/semi analytical solution to show accuracy of the method:

Example 2.7.1 Consider the following one dimensional non-homogeneous fractional equation [93]:

$$\frac{\partial^\alpha u}{\partial t^\alpha}=\frac{\partial^2 u}{\partial x^2}-\frac{\partial u}{\partial x}+\frac{2t^{2-\alpha}}{\Gamma(3-\alpha)}+2x-2, \tag{2.54}$$

with the given conditions

$$u(0,t) = 0, \tag{2.55}$$

$$u(1,t) = 0, \tag{2.56}$$

$$u(x,0) = x^2. \tag{2.57}$$

Clearly, the system given in equations (2.54)-(2.57) is a particular case of model (2.1)-(2.2). The exact solution of equations (2.54)-(2.57) is $u(x,t) = x^2 + t^2$.

By solving this non-linear system, we can find the solution of the problem. For comparison point of view, the problem is solved by taking m=4, and the L_2 and L_∞ errors for $u(x,t)$ are tabulated in Table (2.1) which is defined below

$$L_2 = \| u(x,t_n) - u_m(x,t_n) \|_2 = \sqrt{\int_0^L |u(x,t_n) - u_m(x,t_n)|^2 dx},$$

$$L_\infty = \| u(x,t_n) - u_m(x,t_n) \|_\infty = \max_{\{0<x<L\}} |u(x,t_n) - u_m(x,t_n)|,$$

where $u(x,t_n)$ is the exact solution and $u_m(x,t_n)$ is the approximate solution. Tables (2.1)-(2.2) depict that our proposed solution to the problem of Example (2.7.1) is more accurate than the solution discussed by Uddin and Haq [93] for both the radial basis functions $\phi(r) = r^5$ and $\phi(r) = r^7$. Moreover, figure (2.1) shows the numerical solution with the help of SVFCM and CCM. It is seen from this figure that the results from SVFCM and CCM are nearly same.

Example 2.7.2 Considering the one dimensional reaction-advection diffusion equation by taking $a(u,x,t) = \nu$ and $b(u,x,t) = \tau$ in the model (2.1), where ν, τ are the

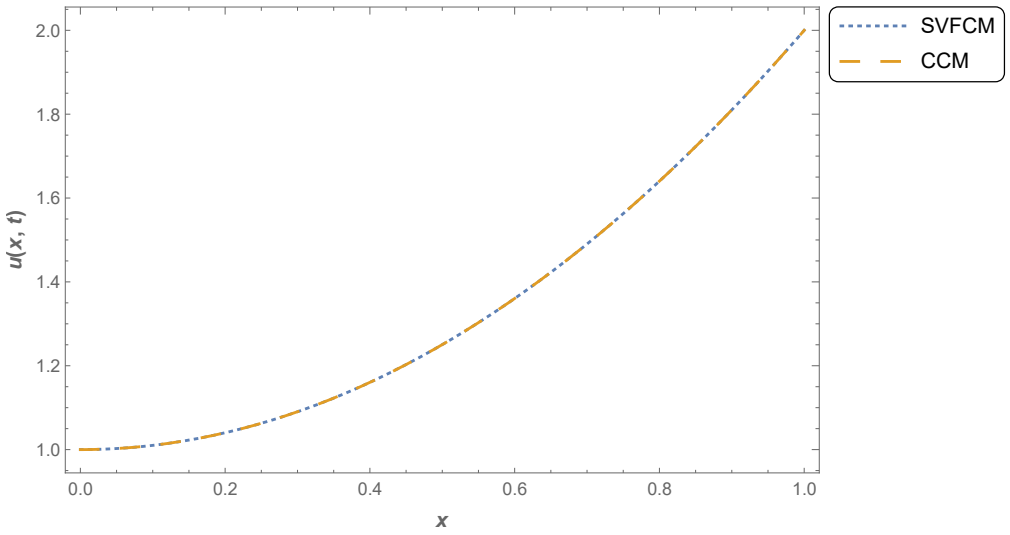

FIGURE 2.1: Numerical solution for example 2.7.1 at $t = 1$ with the help of SVFCM and CCM.

TABLE 2.1: Comparison of L_2 errors of $u(x,t)$ for different values of t at α=0.5 .

t	L_2(our method)	$L_2(r^7)$[93]	$L_2(r^5)$[93]
0.1	6.385×10^{-7}	2.612×10^{-1}	2.613×10^{-1}
0.5	8.075×10^{-6}	1.277×10^{-1}	1.279×10^{-1}
1.0	2.277×10^{-5}	9.120×10^{-2}	9.189×10^{-2}
1.5	5.125×10^{-5}	7.454×10^{-2}	7.597×10^{-2}
2.0	8.629×10^{-5}	6.440×10^{-2}	6.688×10^{-2}

TABLE 2.2: Comparison of L_∞ errors of $u(x,t)$ for different values of t at α=0.5

t	L_∞(our method)	$L_\infty(r^7)$[93]	$L_\infty(r^5)$[93]
0.1	4.7×10^{-7}	6.086×10^{-2}	6.087×10^{-2}
0.5	2.8×10^{-5}	2.958×10^{-2}	2.961×10^{-2}
1.0	1.6×10^{-4}	2.112×10^{-2}	2.122×10^{-2}
1.5	4.7×10^{-4}	1.728×10^{-2}	1.748×10^{-2}
2.0	9.7×10^{-4}	1.495×10^{-2}	1.529×10^{-2}

constants [1]:

$$D^{\alpha}u(x,t) + \tau\frac{\partial u(x,t)}{\partial x} = \nu\frac{\partial^2 u(x,t)}{\partial x^2}, \tag{2.58}$$

with the conditions as:

$$u(x,0) = \exp\left[-\frac{(x-\tau)^2}{4\nu}\right], \tag{2.59}$$

$$u(0,t) = \frac{1}{\sqrt{1+t}}\exp\left[-\frac{((1+t)\tau)^2}{4\nu(1+t)}\right], \tag{2.60}$$

$$u(1,t) = \frac{1}{\sqrt{1+t}}\exp\left[-\frac{(1-(1+t)\tau)^2}{4\nu(1+t)}\right]. \tag{2.61}$$

The analytic solution for this problem at $\alpha = 1$ is given by

$$u(x,t) = \frac{1}{\sqrt{1+t}}exp-\frac{(x-(1+t)\tau)^2}{4\nu(1+t)}. \tag{2.62}$$

Let us define the convergence order (CO) for two successive approximations n_1 and n_2 as

$$CO = \frac{log\left(\frac{R_{n_1}(t)}{R_{n_2}(t)}\right)}{log\left(\frac{n_2}{n_1}\right)},$$

where $R_n(t)$ is the maximum absolute error at time t for the n degree of approximation.

For the problem (2.7.2), table (2.3) is shown at τ=0.25 and ν=0.1 to present the comparison of absolute error between our proposed solution at m=4 and the solutions given in [1] for different m (m=4, 6 and 8). From table (2.3) , it is confirm

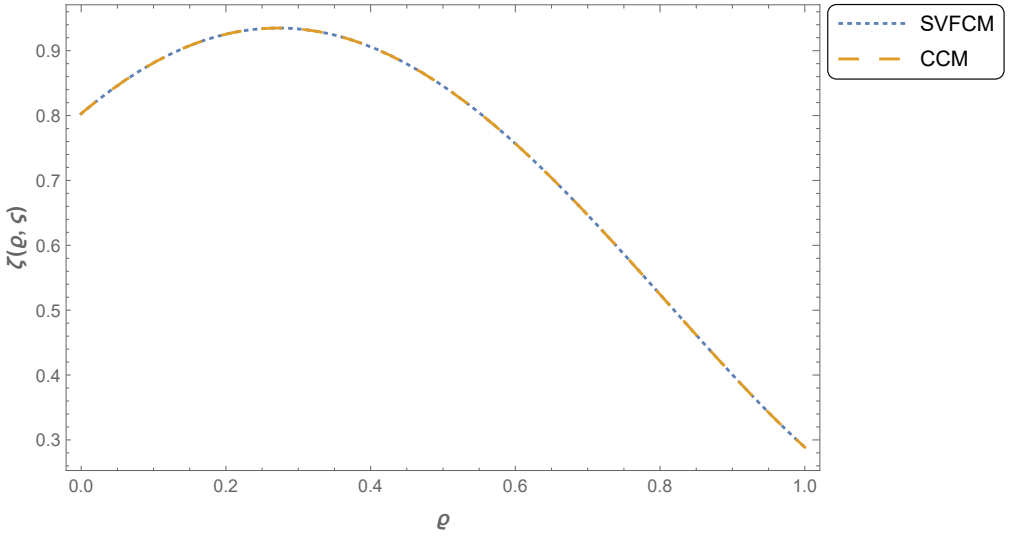

FIGURE 2.2: Numerical solution for example 2.7.2 at $t = 1$ with the help of SVFCM and CCM.

that the solution by proposed scheme at $m = 4$ is better than the solution of [1] at $m = 4$, 6, and 8. Table (2.4) depicts that the proposed scheme has high order of convergence and the order of convergence increases as the degree of appoximating polynomials increase. It is clear from the tables (2.3)-(2.4) that our proposed solution of the problem given in Example (2.7.2) is sufficiently accurate.

Figure (2.3) shows the effect of degree of approximating polynomial (m) on the $log_{10}|error|$ of $u(x,t)$ for the Example (2.7.2). From this Figure, it is confirm that the value of $log_{10}|error|$ is continuously decreasing as we increase the degree of approximating polynomial. Therefore, our proposed solution to the problem converges rapidly to exact solution as m increses. Also the numerical solution is presented in Figure (2.2) with the aid of SVFCM and CCM.

TABLE 2.3: Comparison of absolute error between our solution and solution given in [1] for Example (2.7.2)

Time	m=4 (our method)	m=4 [1]	m=6 [1]	m=8 [1]
0.1	3.02811×10^{-4}	6.67039×10^{-2}	3.41577×10^{-3}	1.37383×10^{-3}
0.2	9.12088×10^{-5}	4.33799×10^{-2}	3.59760×10^{-3}	8.81477×10^{-4}
0.3	8.21903×10^{-6}	3.12633×10^{-2}	3.15220×10^{-3}	5.22709×10^{-4}
0.4	5.29386×10^{-5}	2.48122×10^{-2}	2.68129×10^{-3}	2.21051×10^{-4}
0.5	6.85119×10^{-5}	2.02145×10^{-2}	2.25369×10^{-3}	6.20983×10^{-5}
0.6	6.81041×10^{-5}	1.53190×10^{-2}	1.81808×10^{-3}	6.98557×10^{-5}
0.7	5.90053×10^{-5}	9.58834×10^{-3}	1.41291×10^{-3}	2.41276×10^{-4}
0.8	4.54033×10^{-5}	4.06707×10^{-3}	1.16105×10^{-3}	3.38745×10^{-4}
0.9	2.97423×10^{-5}	1.35780×10^{-3}	1.06073×10^{-3}	3.22167×10^{-4}

TABLE 2.4: The convergence order for Example (2.7.2) at t=1 and α=1.

m	L_∞ error	CO	L_2 error	CO
2	1.95683×10^{-3}	-	1.18695×10^{-3}	-
4	3.59778×10^{-4}	1.6577	2.97496×10^{-4}	1.3544
6	6.47853×10^{-5}	1.8238	5.89563×10^{-5}	1.7219
8	9.85673×10^{-6}	1.9392	8.97365×10^{-6}	1.9387

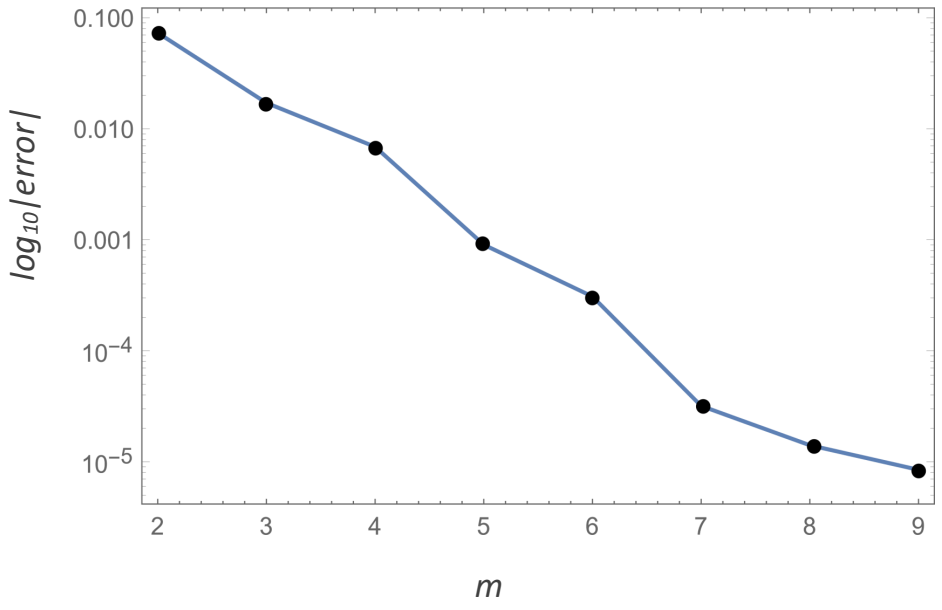

FIGURE 2.3: Plot of $log_{10}|error|$ vs. degree of polynomial m at t=1 and $\alpha = 1$.

After the discussion of validation and accuracy of the proposed method, this scheme is applied to the following two particular cases of the space time-fractional order advection reaction diffusion equations (2.1)-(2.2) to demonstrate the behavior of solute concentration profiles:

Case 1. In this case, we consider a non-conservative term $f(u,x,t) = \lambda u(1-u)(u-1)$ in the model (2.1) with the following conditions:

$$u(x,0) = x^2(1-x),$$
$$u(1,t) = 0,$$
$$u(0,t) = 0.$$

Figures (2.4)-(2.6) demonstrate the concave downward solute concentration profiles and the effects of α and γ on these profiles for the non-conservative system as given in Case 1. Figures (2.4)-(2.6) show that the concentration profiles decrease as α and β increase, and the concentration profiles for fractional cases shift towards the standard case (integer-order derivative, i.e., α=1, β=2) as we enhance the value of α and β. Figure (2.6) depicts that the concentration profile in the domain increases as the value of γ improves. Moreover, we also observe that the concentration profile corresponding to the fractional value of γ moves towards the concentration profile corresponding to γ=1 as the parameter γ increases.

Case 2. In equation (2.1), we consider the following conservative term

$$f(u,x,t) = e^{-2t}\left(2(x^{\gamma} - x^{\beta}) - (\beta)! + \frac{\Gamma(\beta+1)}{\Gamma(\beta-\gamma+1)}x^{\beta-\gamma} - \gamma!\right),$$

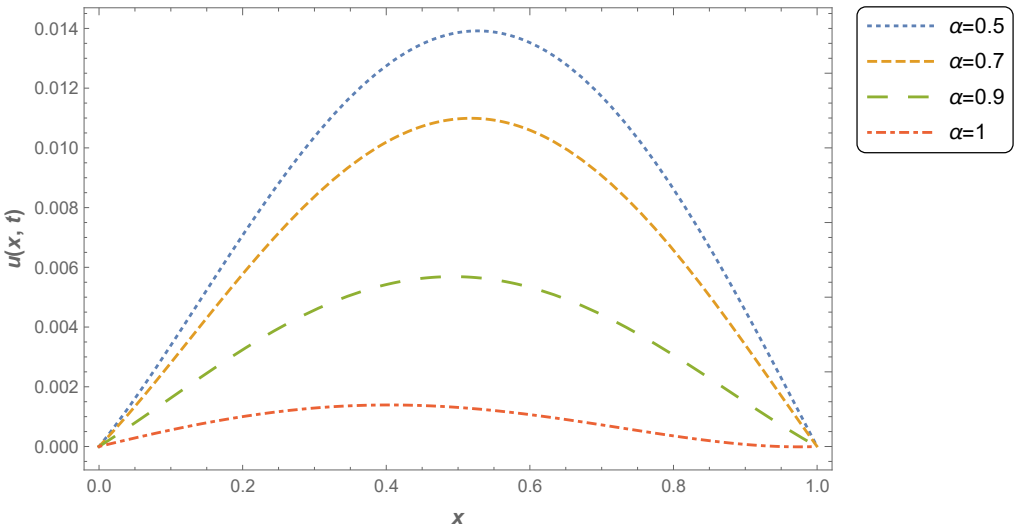

FIGURE 2.4: Plots of solute concentration $u(x,t)$ vs. x for non-conservative system with different value of α at β=1.5, γ=0.7, λ=1 and t=0.5.

with the following conditions:

$$u(0,t) = 0,$$

$$u(1,t) = 0,$$

$$u(x,0) = x^{\beta} - x^{\gamma}.$$

Figures (2.7)-(2.9) present concave upward solute concentration profiles to show the effect of the parameters α, β and γ on these profile for conservative system as mentioned in Case 2. From these figures, it is found that the variation of α on the concentration profile is less effective than the variation of β and γ. As we increase the fractional order derivatives, the profiles of solute concentrations associated with the fractional parameter α, β and γ converge to the concentration profiles corresponding to α=1, β=2 and γ=1 (Standard case).

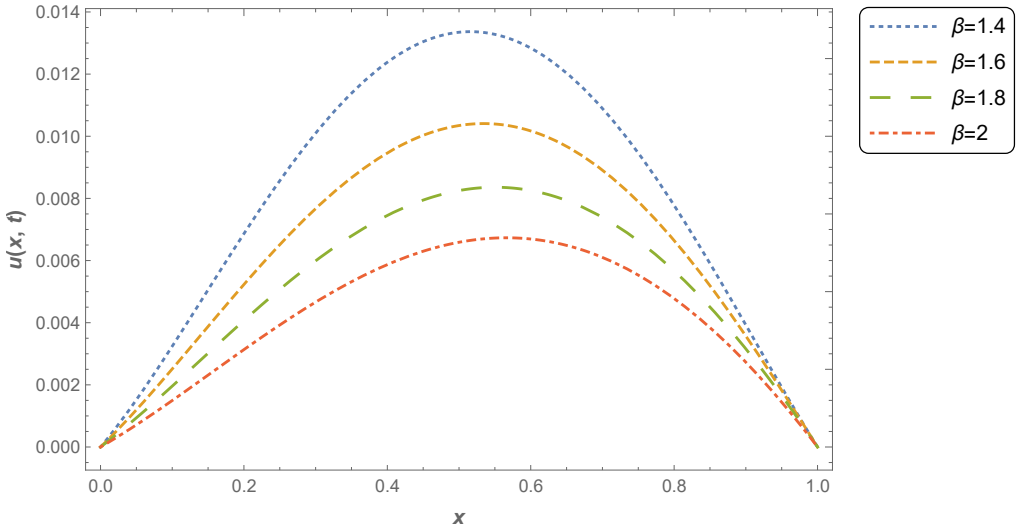

FIGURE 2.5: Plots of solute concentration $u(x,t)$ vs. x for non-conservative system with different value of β at α=0.7, γ=0.8, λ=1 and t=0.5.

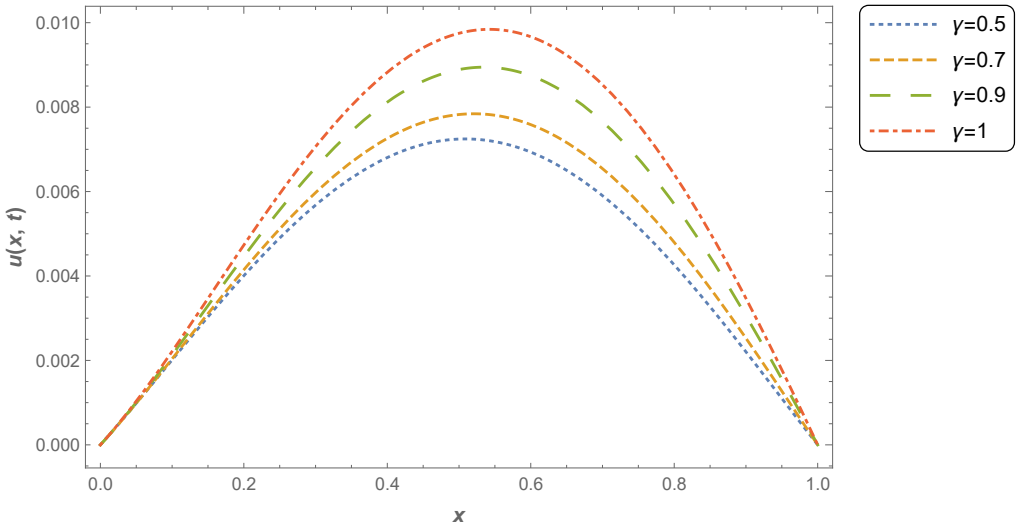

FIGURE 2.6: Plots of solute concentration $u(x,t)$ vs. x for non-conservative system with different value of γ at α=0.8, β=1.6, λ=1 and t=0.5.

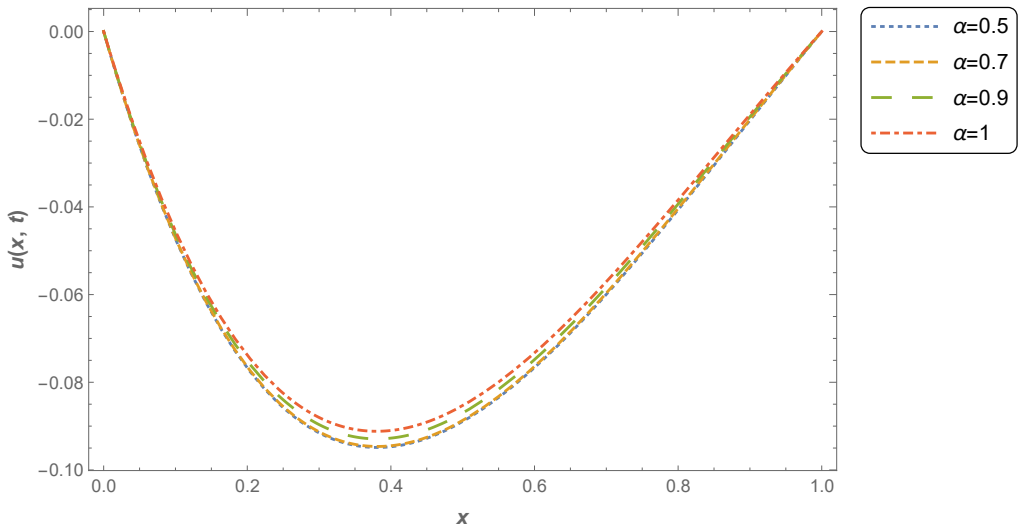

FIGURE 2.7: Plots of solute concentration $u(x,t)$ vs. x for conservative system with different value of α at β=1.5, γ=0.7 and t=0.5.

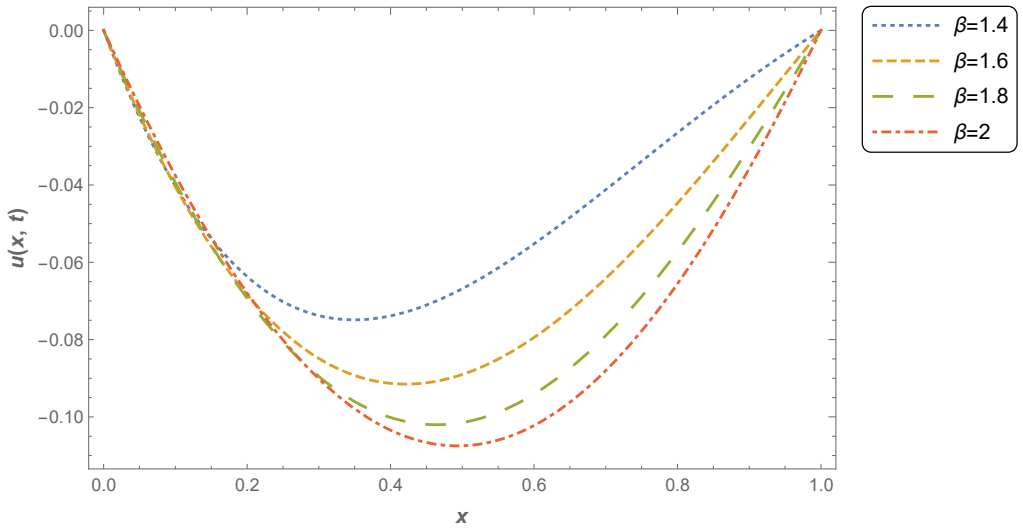

FIGURE 2.8: Plots of solute concentration $u(x,t)$ vs. x for conservative system with different value of β at α=0.7, γ=0.8 and t=0.5.

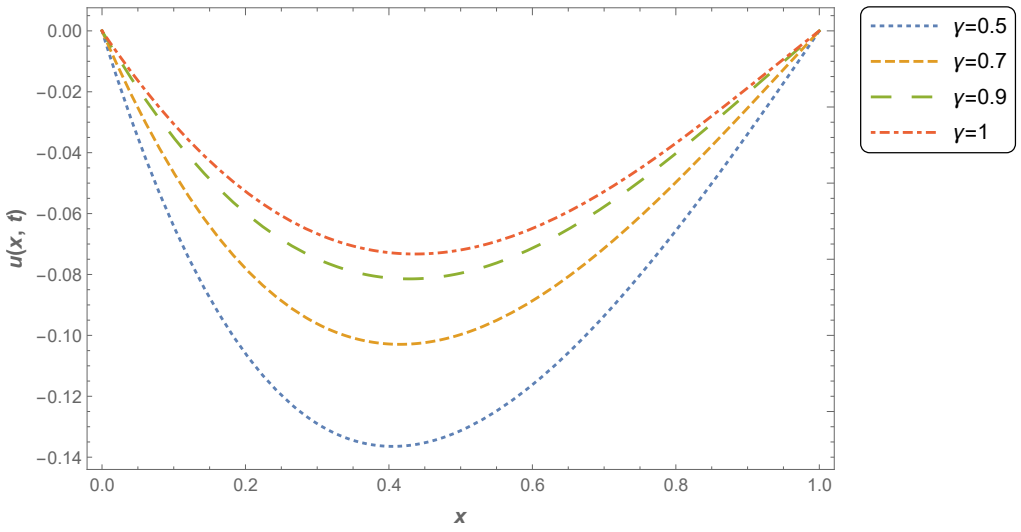

FIGURE 2.9: Plots of solute concentration $u(x,t)$ vs. x for conservative system with different value of γ at α=0.8, β=1.6 and t=0.5.

2.8 Conclusion

In this chapter, the approximations of fractional time derivative and space derivative are considered with the aid of non-standard finite difference scheme and Vieta-Fibonacci polynomials, respectively to solve the non-linear fractional-order space-time reaction advection-diffusion equation. The stability and convergence of the proposed scheme are established theoretically. From this study, it is found that presented scheme is unconditionally stable and the convergence order with respect to time is $O(\Delta x^{2-\alpha})$. Several numerical examples are used to show the validity of this approach, and it is observed that our solution is more accurate than the other available schemes given in [84], [93] and [1]. It is seen from the example that the accuracy of the scheme increases as the degree of approximating polynomials rises. It is also shown that SVFCM and CCM produces the same results. Finally, it is observed that the proposed approach is a simpler and efficient tool to solve the nonlinear fractional-order advection reaction diffusion equations. Moreover, this approach will be helpful to handle various problems arising in the different fields

of science and industries. Further, for both the conservative and non-conservative system, the parameters α, β, and γ affects the concentration profiles, and all the concentration profiles shift towards integer-order case from fractional-order when we increase α or/and β or/and γ.

From the future point of view, the researchers can extend the proposed scheme to solve the various linear and nonlinear problems in two and three dimensions with different kinds of boundary conditions. The researcher can implement the proposed scheme on various problems from the different fields, like heat and mass transfer, fluid flow in porous media, bio-mechanics, gas dynamics, etc. Further, the researchers can develop other algorithms based on the proposed scheme by taking different polynomials like Legendre, Laguerre, Genonacchi, etc.

****